Resonant Mechanisms of Inelastic Light Scattering by Low-Dimensional Electron Gases

B. Jusserand,[1] M. N. Vijayaraghavan,[2,*] F. Laruelle,[2] A. Cavanna,[2] and B. Etienne[2]

[1]*CDP, CNET-CNRS, 196 Avenue Henri Ravera, BP 107, 92225 Bagneux Cedex, France*

[2]*L2M, CNRS, 196 Avenue Henri Ravera, BP 107, 92225 Bagneux Cedex, France*

(Received 22 February 2000)

The contribution of elementary excitations in low-dimensional electron gases to resonant inelastic light scattering is found to be determined by interband transitions involving states at *specific* wave vectors. In modulation-doped GaAs/GaAlAs quantum wells, we detect only the single-particle excitations (SPE) at resonances with electron-hole transitions at the Fermi wave vector, and only plasmons at resonances with zone-center excitons. The plasmon cross section is comparable to the SPE when double electronic resonance is achieved by tuning the plasmon energy to a valence subband separation.

PACS numbers: 73.20.Mf, 78.30.Fs, 78.66.Fd

The physics of interacting electron gases at low dimensions concerns a large class of materials systems such as organic and inorganic naturally one-dimensional (1D) conductors, edge states in the fractional quantum Hall regime, metallic carbon nanotubes, and doped semiconductor quantum wires. While the Fermi liquid theory successfully describes 2D interacting electron systems and predicts coexisting quasiparticules and collective excitations across the Fermi surface, it no longer applies to 1D systems. For 1D conductors, the adequate theoretical scheme is the Luttinger liquid whose distinctive features are the disappearance of any quasiparticle excitation and the power law behavior of physical quantities across the Fermi surface [1]. Various experimental methods have been applied to obtain evidence of these specific differences. Power law variations of conductivity with temperature were recently reported in transport experiments in semiconductor wires [2] and in carbon nanotubes [3], as well as in the optical conductivity of organic materials [4]. Photoemission studies of naturally 1D conductors such as $Li_{0.9}Mo_6O_{17}$ have revealed the absence of step in the occupation function at the Fermi energy [5]. Surprisingly, however, early Raman spectroscopy results on doped semiconductor quantum wires were successfully interpreted within the Fermi model [6]. Raman scattering is very powerful to study electronic excitations close to the Fermi surface since quasiparticule excitations [often denoted single-particle excitation (SPE)] and collective modes (plasmons) display distinctive polarization selection rules. Sassetti and Kramer [7] recently showed that the results of Ref. [6] could be reinterpreted within the Luttinger model. Unambiguous observation of the disappearance of SPE lines in the Raman signal in a strictly 1D system thus remains a challenging goal.

One must, however, realize that the observation of SPE at 2D is already in contradiction to the standard Fermi liquid theory of the electronic Raman cross section [8], in which the SPE contribution is almost fully screened. Nevertheless, there have been several experimental reports [9] of the observation of intense SPE lines in 2D electron gases. Large variations of the line intensities with the incident laser frequency have been demonstrated, showing the importance of the resonant mechanisms negelected in the standard theory. Moreover, important variations from sample to sample still remain to be understood, possibly in terms of disorder.

In a recent Letter [10], Das Sarma and Wang presented a significant advance in this old puzzling problem. They show that intense SPE lines are predicted in the absence of disorder, due to strong resonance conditions. This statement has stimulated us to perform a systematic study of the resonance profile of both SPE and plasmon lines in a high-quality two-dimensional electron gas (2DEG). We report in this Letter on the observation of Raman resonances associated with both SPE and plasmon lines. We demonstrate that the different excitations resonate at completely different and mutually exclusive interband virtual transitions: plasmons at zone-center excitons associated with empty conduction subbands, and SPE at Fermi edge transitions associated with the fundamental occupied conduction subband. We confirm experimentally the main theoretical prediction of Ref. [10] and we show that resonant Raman scattering by SPE is well described within the electron density fluctuation mechanism, while plasmon lines are not observed at the same resonances. In addition we observed novel behaviors for the plasmon cross section, namely, its strong variation as a function of the scattering wave vector. A decrease of this cross section could be understood in terms of Landau damping, because the plasmon energy goes closer to the SPE continuum at larger wave vector. We observe the opposite variation: the plasmon cross section increases with increasing wave vector. Moreover, we observed for some samples a very strong increase of the plasmon cross section, without significant change of the density, after etching the sample surface. We show that other resonant mechanisms, not included in Ref. [10], are essential to obtaining a comprehensive understanding of our experiments and that these mechanisms are possibly very sensitive to potential fluctuations in the structures.

We have investigated two different samples, both one-side modulation-doped GaAs/AlAs 18-nm-wide quantum wells, with the same spacer layer thickness (20 nm) and

 0031-9007/00/85(25)/5400(4)$15.00

the same distance to the surface (85 nm). The Si delta-doping dose in sample A (1.0×10^{12} cm^{-2}) has been adjusted close to the minimum amount necessary to saturate both the midgap surface states and quantum well density, in order to minimize potential fluctuations due to remote ionized impurity scattering. The corresponding Hall density and mobility amount to 3×10^{11} cm^{-2} and 2×10^5 cm^2/V · s in the dark and 7×10^{11} cm^{-2} and 2×10^6 cm^{-2}/V · s after strong illumination. In sample B, we used a larger Si dose (3.7×10^{12} cm^{-2}), and the Hall density and mobility then amount to 4×10^{11} cm^{-2} and 9×10^5 cm^2/V · s in the dark and 6.9×10^{11} cm^{-2} and 4.5×10^6 cm^2/V · s after strong illumination. The Raman experiments were performed on the samples immersed in superfluid helium with a typical power density of 10 W/cm^2 in close resonance to the lowest 2D transitions in the 2DEG.

The resonance data for sample A are shown in Figs. 1a and 1b for incident energies at about 1.57 and 1.55 eV, respectively, and for a fixed incidence angle (50°) corresponding to an in-plane wave vector transferred to the electron gases equal to 1.2×10^5 cm^{-1}. In Fig. 1a the energy of the Raman lines is slightly above the E_2H_1 exciton line observed in luminescence (at 1.5578 eV in this sample), while in Fig. 1b they are close to the Fermi edge observed in luminescence. Two Raman lines are observed. At a lower energy shift (2.8 meV at this angle), an asymmetric line with a linear dispersion (not shown) is assigned to single-particle excitations. From the slope of the dispersion, we extract a density of 7×10^{11} cm^{-2}. At higher energy shift (8.5 meV), a plasmon line is recorded, with a quasi-square-root dispersion (not shown). It is remarkable that the plasmon line is observed only in a very limited range of incident energies between 1.573 and 1.575 eV and displays a very sharp resonance in this range. The SPE resonances (about 1.570 and 1.545 eV) are broader.

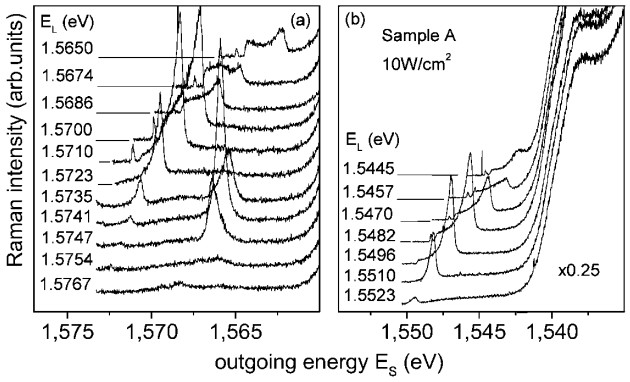

FIG. 1. Dependence of the Raman spectra on the outgoing energy, taken in sample A at fixed angle of incidence (50°), above the E_2H_1 luminescence line (a) or above the luminescence Fermi edge (b). The Raman curves have been shifted vertically for clarity. The corresponding laser energy is given for each curve.

We stress that the resonances of both excitations appear at different energies, either in the ingoing or in the outgoing channels, i.e., either when the incident (E_L) or the scattered (E_S) photon energies corresponding to the maxima of the resonances are compared.

These experimental observations cannot be fully understood based on the theoretical description from Ref. [10], which predicts that SPE lines and plasmons should resonate at the same energy. In order to understand this novel result, we compare the Raman resonance profiles to the luminescence and the photoluminescence excitation (PLE) curves in the same sample. In Fig. 2a, steps in the PLE spectrum correspond to vertical transitions beyond k_F between the occupied subband E_1 and the valence subbands H_1, L_1, and H_2 (labeled with a star) while peaks correspond to zone-center excitonic resonance between the empty conduction subband E_2 and the same valence subbands. Their assignment has been checked from circular polarization measurements and their energies fairly agree with the calculations of Ref. [11]. In the same graph, we have plotted Raman intensities as a function of the outgoing energy because the peak resonance energy shifts when the Raman shift is changed, while the laser position remains fixed. From comparison with the PLE, we deduce that the two SPE resonances coincide with two steps associated with $E_1L_1^*$ and $E_1H_2^*$, respectively, i.e., that the resonance mechanism involves the $k = k_F$ states in the E_1 occupied subband. The corresponding resonance is fairly narrow with a typical width of 3.7 meV. The single plasmon resonance is much narrower, with a typical width smaller than 1 meV. Its maximum coincides with the E_2L_1 excitonic resonance observed in PLE. It

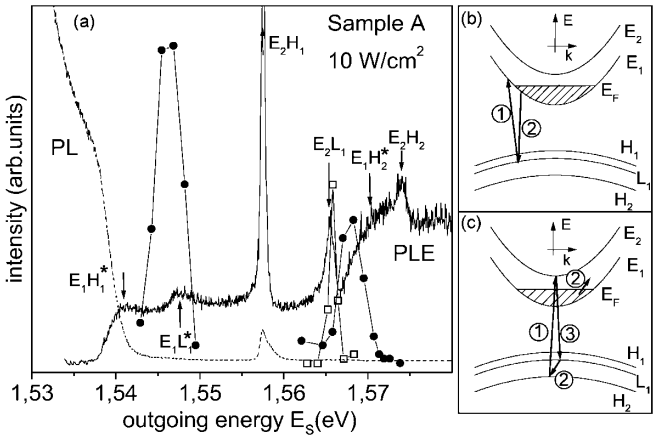

FIG. 2. (a) Comparison between the luminescence (dashed line) and the PLE (solid line) with the Raman intensities plotted as a function of the scattered energy for the plasmon (open squares) and the SPE (full circles). The assignment of the interband transitions is given. (b),(c) Valence and conduction subband dispersion with schematic representations of the Raman mechanisms invoked for the SPE resonance [(b) electron density fluctuations] and for the plasmon resonance [(c) double excitonic resonance].

follows from these novel observations that completely different mechanisms have to be considered to quantitatively describe the SPE and the plasmon resonances, respectively.

The SPE resonance close to Fermi edge transitions can be explained within the electron density fluctuation mechanism [10] in which the photon couples directly to the Fermi sea. As shown in Fig. 2b, an electron is promoted from the valence subband to an empty state above E_F (step 1). Then an electron below the Fermi level recombines with the remaining hole in the valence band (step 2). Within this mechanism, the Raman cross section is difficult to evaluate exactly. Assuming nonresonant conditions [8], drastic approximations can be made: the transition energy between the involved conduction and valence states is assumed to be the same for any couple of states, and the quasistatic approximation is made: $E_L = E_S$. By using fluctuation-dissipation theory, the Raman cross section is then proportional to the many-body dielectric response function of the electron gas. SPE lines are very strongly screened in these conditions.

Using more sophisticated treatments of the same mechanism, it was shown recently [10] that SPE scattering can even overcome plasmon scattering at very strong electronic resonance. Our data indeed confirm that SPE dominates in these conditions. Moreover we verify the theoretical predictions that the resonance curve peaks when the *scattered* energy equals the transition at k_F, either $E_1L_1^*$ or $E_1\mathrm{H}_2^*$ and exhibits a narrow width reflecting the small energy range of allowed initial states. We have not been able to detect any plasmon scattering based on the same mechanism, i.e., when the laser is adjusted such that the plasmon line coincides with a Fermi edge transition. This indicates that the resonant plasmon scattering is at least 2 orders of magnitude smaller than the SPE, while ratios of the order of unity are emphasized in Ref. [10]. One must, however, stress that (i) a much smaller ratio appears in Fig. 4 of Ref. [10] in very strong resonance, actually for 1D gases, and (ii) no predictions are given for the absolute resonance curves and it remains impossible to estimate whether the absolute resonant curve for plasmons is consistent with our observations.

On the other hand, the strong and narrow resonance of the plasmon peak cannot be explained within the same mechanism, and one has to look for another light scattering process. Let us first present a detailed experimental description of this resonance in sample B, after a 45-nm wet-etching of the GaAlAs barrier. The results on the as-grown sample will be further discussed below. All of the Raman properties in the etched sample compare well with those in sample A: a narrow resonance is recorded when the outgoing photon coincides with the E_2L_1 exciton resonance in PLE. At this particular angle, the resonance energy moreover coincides with the $E_2\mathrm{H}_2$ excitonic resonance when the incoming photon is considered. This feature, novel in the context of electronic excitations, was already reported for optical phonons in quantum wells [12] as a double resonance, when the LO phonon energy equals an intersubband energy splitting in the conduction band. Here, the intrasubband plasmon energy equals a valence subband separation (between L_1 and H_2) and we take advantage of the tunability of this energy with the angle of incidence to fully explore the double resonance behavior.

We show, in Fig. 3a, Raman spectra obtained at several angles of incidence on the 45-nm-etched sample B and with the incident laser energy optimized for maximum intensity for each wave vector. This maximum intensity is strongly varying with angle, i.e., with the plasmon energy. In Fig. 3c, we show the overall variation of the plasmon intensities as a function of the incident laser energy for a different angle of incidence. To quantitatively analyze this data, we use a mechanism introduced in Ref. [13] to analyze resonance profiles of intersubband excitations. It relies on excitonic intermediate states coupled to plasmons via Coulomb interactions. As shown in Fig. 2c, the incident photon creates a near-zone-center exciton between the empty valence and the conduction bands (step 1). A transition to a lower energy exciton, corresponding to a different valence subband, goes with the plasmon creation (step 2) and is followed by the recombination of this new exciton (step 3). Within this model, the dominant term in the Raman cross section writes

$$R = \left| \frac{C}{(E_1^X - E_L + id_1)(E_2^X - E_S + id_2)} \right|^2,$$

where E_1^X and E_2^X are two different excitonic transitions with a linewidth d_1 and d_2, respectively, and C contains matrix elements. The first factor in the denominator

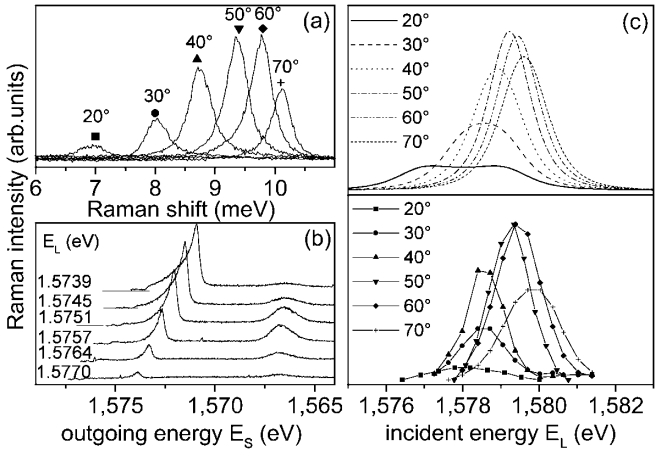

FIG. 3. (a) Raman spectra due to plasmons in the etched sample B at the resonance peak for several incidence angles. (b) Dependence of the Raman spectra on the outgoing energy, taken in sample B (as grown) at a fixed angle of incidence (50°). (c) Variation of the Raman intensity of the plasmon in the etched sample B close to double resonance. The symbols correspond to measured intensities (bottom curves) and the lines to calculated intensities (top curves), both plotted as a function of the incident energy.

corresponds to the incoming channel while the second one is associated with the outgoing channel. In Fig. 3c, the resonance profiles calculated for different experimental angles using $E_1^X = 1.5793$ eV, $E_2^X = 1.5698$ eV, and $d_1 = d_2 = 1$ meV are compared to the experiment. They reproduce well the main trends of the experimental results: (i) The maximum intensity rapidly decreases when the double resonance is detuned. (ii) When the wave vector is changed, the peak resonance energy shift is smaller than the corresponding Raman shift due to the mixing of the two (incoming and outgoing) channels involved in the Raman cross section. These fitting parameters agree well with the parameters of the two excitonic transitions to which we assign the double resonance: E_2H_2 ($E = 1.5790$ eV, $d = 0.7$ meV) and E_2L_1 ($E = 1.5694$ eV, $d = 0.7$ meV). Though intensities calculated within our model decay less rapidly than measured ones at large detunings, the assignment of the observed plasmon resonance to a double excitonic mechanism is fully justified with the unique features of a very strong intensity and a very narrow range of observation.

Let us now come back to the effect of etching on sample B. We have observed a significant modification of the plasmon lines due to etching, while the other optical properties of the sample are only slightly affected. The SPE resonance remains the same before and after etching, while the plasmon resonances display the narrow and intense behavior described previously only after etching. As shown in Fig. 3b, the observations are quite different before etching. The plasmon line is poorly resolved and appears as an increase of the small hot luminescence feature at E_2L_1, when it goes through. By using the previous model with the same value of the constant C, we reproduce the results in almost double resonance by taking $d_1 = d_2 = 1.3$ meV instead of 1.0 meV. Such an exciton broadening is not observed in the PLE spectra, which remain unaffected by etching, except for a rigid shift. The origin of this moderate additional broadening and of its dramatic consequences on the plasmon Raman line double resonance remains to be determined. When noting that the fitted broadening parameters of the etched sample data were larger than the excitonic widths (0.7 meV), we propose plasmon damping due to Coulomb interaction with charged impurities as a possible mechanism to explain the observed additional broadening, and we tentatively assign the strong variations of the plasmon resonances to a change of the parallel charge distribution either with the initial doping dose or, equivalently, with the surface etching.

In conclusion, we have presented an overall experimental determination of the resonant light scattering cross section by electronic excitation in high mobility 2DEGs. We confirm that the recently published proposal [10] in which the electron density fluctuation mechanism induces strong single-particle excitation scattering at resonance, is experimentally verified in very low disorder samples. We show furthermore that plasmon scattering due to this mechanism is not detectable at resonance but reaches intensities comparable to SPE when double excitonic resonance is achieved. This double resonance fully explains the wave vector dependence of the plasmon cross section observed in 2DEGs. As anticipated in Ref. [10], resonant mechanisms which are already of paramount importance in 2D, as demonstrated here, should also play a determinant role in 1D systems. The experimental advances presented in this Letter should allow one to draw firm conclusions on the 1D behavior in future electronic Raman scattering studies of semiconductor quantum wires [14]. This approach could also be extended to other 1D conductors.

M. N. Vijayaraghavan acknowledges IFCPAR Grant No. 1514-1 for financial support. We acknowledge partial financial support for this work from "Conseil Régional d'Ile de France" through a SESAME grant.

*Present address: Department of Physics, Indian Institute of Science, Bangalore, India.

[1] H. Schulz, Phys. Rev. Lett. **71**, 1864 (1993); J. Voit, Rep. Prog. Phys. **58**, 977 (1995).
[2] O. M. Auslaender, A. Yacoby, R. de Picciotto, K. W. Baldwin, L. N. Pfeiffer, and K. W. West, Phys. Rev. Lett. **84**, 1764 (2000).
[3] M. Bockrath, D. H. Coldren, J. Lu, A. G. Rinzler, R. E. Smalley, L. Balents, and P. L. McEuen, Nature (London) **398**, 598 (1999).
[4] V. Vescoli, L. Degiorgi, W. Henderson, G. Grüner, K. P. Starkey, and L. K. Montgomery, Science **281**, 1181 (1998).
[5] J. D. Denlinger *et al.,* Phys. Rev. Lett. **82**, 2540 (1999).
[6] A. R. Goñi *et al.,* Phys. Rev. Lett. **67**, 3298 (1991).
[7] M. Sassetti and B. Kramer, Phys. Rev. Lett. **80**, 1485 (1998).
[8] G. Abstreiter, M. Cardona, and A. Pinczuk, in *Light Scattering in Solids IV,* edited by M. Cardona and G. Güntherodt (Springer-Verlag, Berlin, 1984), p. 4; D. C. Hamilton and A. L. MacWhorter, in *Light Scattering in Solids,* edited by G. B. Wright (Springer-Verlag, Berlin, 1969), p. 309.
[9] In addition to Refs. [1–10] in [10], see also G. Fasol, N. Mestres, H. P. Hughes, A. Fischer, and K. Ploog, Phys. Rev. Lett. **56**, 2517 (1986); B. Jusserand, D. Richards, H. Peric, and B. Etienne, Phys. Rev. Lett. **69**, 848 (1992).
[10] S. Das Sarma and D. W. Wang, Phys. Rev. Lett. **83**, 816 (1999).
[11] M. H. Meynadier, J. Orgonasi, C. Delalande, J. A. Brum, G. Bastard, M. Voos, G. Weimann, and W. Schlapp, Phys. Rev. B **34**, 2482 (1986).
[12] D. A. Kleinman, R. C. Miller, and A. C. Gossard, Phys. Rev. B **35**, 664 (1987).
[13] G. Danan, A. Pinczuk, J. P. Valladares, L. N. Pfeiffer, K. W. West, and C. W. Tu, Phys. Rev. B **39**, 5512 (1989).
[14] Preliminary results are discussed in F. Perez, B. Jusserand, and B. Etienne, Physica (Amsterdam) **7E**, 521 (2000).